ORIGINAL ARTICLE

Hong Xu · Yi Liang · Peng Zhang · Fen Du
Bing-Rui Zhou · Jun Wu · Jian-Hong Liu
Zhi-Gang Liu · Liang-Nian Ji

Biophysical studies of a ruthenium(II) polypyridyl complex binding to DNA and RNA prove that nucleic acid structure has significant effects on binding behaviors

Abstract The interactions of a metal complex [Ru (phen)$_2$PMIP]$^{2+}$ {Ru = ruthenium, phen = 1,10-phenanthroline, PMIP = 2-(4-methylphenyl)imidazo[4,5-f]1,10-phenanthroline} with yeast tRNA and calf thymus DNA (CT DNA) have been investigated comparatively by UV-vis spectroscopy, fluorescence spectroscopy, viscosity measurements, isothermal titration calorimetry (ITC), as well as equilibrium dialysis and circular dichroism (CD). Spectroscopic studies together with ITC and viscosity measurements indicate that both binding modes of the Ru(II) polypyridyl complex to yeast tRNA and CT DNA are intercalation and yeast tRNA binding of the complex is stronger than CT DNA binding. ITC experiments show that the interaction of the complex with yeast tRNA is driven by a moderately favorable enthalpy decrease in combination with a moderately favorable entropy increase, while the binding of the complex to CT DNA is driven by a large favorable enthalpy decrease with a less favorable entropy increase. The results from equilibrium dialysis and CD suggest that both interactions are enantioselective and the Δ enantiomer of the complex may bind more favorably to both yeast tRNA and CT DNA than the Λ enantiomer does, and that the complex is a better candidate for an enantioselective binder to yeast tRNA than to CT DNA. Taken together, these results indicate that the structures of nucleic acids have significant effects on the binding behaviors of metal complexes.

Keywords Binding affinity · Calorimetry · Fluorescence · Molecular recognition · Thermodynamics

Abbreviations bpy: 2,2′-Bipyridine · CD: Circular dichroism · CT DNA: Calf thymus DNA · DMSO: Dimethyl sulfoxide · DPPZ: Dipyrido[3,2-*a*:2′,3′-*c*]phenazine · IL: Intraligand · ITC: Isothermal titration calorimetry · MCP: 2-(3-Chlorophenyl) imidazo[4,5-f]1,10-phenanthroline · MLCT: Metal-to-ligand charge transfer · NMR: Nuclear magnetic resonance · m/z: Ratio of mass to charge · phen: 1,10-Phenanthroline · PMIP: 2-(4-Methylphenyl)imidazo[4,5-f]1, 10-phenanthroline · Ru: Ruthenium · UV-vis: Ultraviolet and visible

H. Xu · Y. Liang (✉) · P. Zhang · F. Du · B.-R. Zhou · J. Wu
State Key Laboratory of Virology, College of Life Sciences,
Wuhan University,
Wuhan 430072, China
E-mail: liangyi@whu.edu.cn
Fax: +86-27-68752560

H. Xu · J.-H. Liu · Z.-G. Liu
Department of Chemistry and Biology, Normal College,
Shenzhen University,
Shenzhen 518060, China

H. Xu
State Key Laboratory of Coordination Chemistry,
Nanjing University,
Nanjing 210093, China

L.-N. Ji
Key Laboratory of Gene Engineering of Ministry of Education,
Zhongshan University,
Guangzhou 510275, China

Introduction

During the past decade, the interaction of metal complexes including ruthenium Ru(II) complexes with DNA has attracted much attention, and the use of these complexes as probes of DNA structure and sites has proven to be quite fruitful [1–5]. Some new theoretical calculations and technologies, such as density functional theory method, picosecond time-resolved resonance Raman spectroscopy, and femtosecond linear dichroism, have been widely used to study the strength, geometries, and modes of Ru(II) complexes binding to DNA [6–13]. In general, Ru(II) complexes bind with DNA in a non-covalent interaction fashion, such as electrostatic binding for cations, groove binding for large ligands [14], intercalative binding for planar ligands, and partial

intercalative binding for incompletely planar ligands [15, 16]. On the other hand, a considerable amount of new information for RNA–metal complex interactions has also emerged. Metal complexes are usually used as catalysts of RNA hydrolysis cleavage [17], shape-selective probes of RNA tertiary structure [18], agents of RNA oxidation cleavage [19], and recognition of mismatches in RNA [20]. Also, the binding mode and enantioselectivity for the interaction of a Ru(II) complex with yeast tRNA has been investigated by spectroscopic methods [21], and the anti-HIV activity and enantiomeric diversity of eilatin Ru(II) complexes binding to RNA [22, 23] have been reported.

Although some experimental investigations on RNA–metal complex interactions have been carried out during the past decade as described above, many questions still need to be answered for a better understanding of the mechanism and the biological implications of the interactions. One of the questions is that how the structures of nucleic acids affect the binding behaviors of metal complexes. It is well known that yeast tRNA is different from calf thymus DNA (CT DNA) not only in composition of bases, but also in structure. CT DNA is B-form configuration, while yeast tRNA has an A-form configuration with a L-shaped tertiary structure. Therefore, a comparative study of the interactions of Ru(II) complexes with yeast tRNA and CT DNA in binding mode, binding strength, driving force, and enantioselectivity will be really important for understanding the mechanism of the interactions and the biological impact of Ru(II) complexes.

Isothermal titration calorimetry (ITC) is an important tool for the study of both thermodynamic and kinetic properties of biological macromolecules by virtue of its general applicability and high precision, as shown by recent developments [24–27]. Recently, this method has yielded some useful thermodynamic data on drug-RNA/DNA interactions [28–32]. However, information on thermodynamics of the binding of Ru(II) complexes to both RNA and DNA, which is necessary for a thorough understanding of the mechanism, is eagerly awaited.

In a previous publication from this laboratory [32], the binding of (1,10-phenanthroline)-copper complex to CT DNA was investigated by isothermal calorimetry. In this paper, we described a comparative study of the interactions of a Ru(II) complex, $[Ru(phen)_2PMIP]^{2+}$ {phen = 1,10-phenanthroline, PMIP = 2-(4-methylphenyl)imidazo[4,5-f]1,10-phenanthroline} (Fig. 1), with yeast tRNA and CT DNA using UV-vis spectroscopy, fluorescence spectroscopy, viscosity measurements, equilibrium dialysis, circular dichroism (CD), as well as ITC for the first time. Information obtained from this study will be helpful to the understanding of the mechanism of the interactions of Ru(II) complexes with nucleic acids, and should be useful in the development of nucleic acid molecular probes and new therapeutic regents for some diseases related to viruses such as AIDS and SARS.
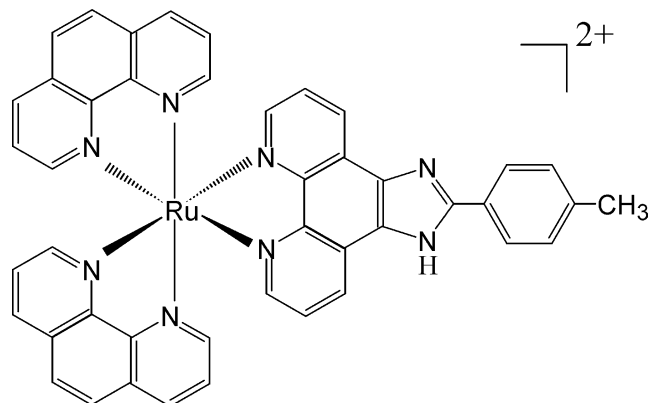

Fig. 1 Structure of complex $[Ru(phen)_2PMIP]^{2+}$

Materials and methods

Synthesis

1,10-Phenanthroline-5,6-dione and cis-$[Ru(phen)_2Cl_2] \cdot 2$-H_2O were prepared according to the literature procedures [33, 34]. PMIP[1,2] was synthesized by a method similar to the one described previously [6]. A mixture of 4-methylbenzaldehyde (3.5 mmol, 0.41 ml), 1,10-phenanthroline-5,6-dione (2.5 mmol, 0.525 g), ammonium acetate (50 mmol, 3.88 g), and glacial acetic acid (10 ml) was refluxed for about 2 h, then cooled to room temperature, and diluted with water (about 25 ml). Dropwise addition of concentrated aqueous ammonia gave yellow precipitates, which were collected and washed with water. The crude products were purified by silica gel filtration (60–100 mesh, ethanol). The principal yellow band was collected. The solvent was removed by rotary evaporation, and the products were collected and dried at 50°C in vacuo. Yield, 0.588 g, 76%.

Complex $[Ru(phen)_2PMIP](ClO_4)_2 \cdot H_2O$ (red) was prepared by the following method. A mixture of cis-$[Ru(phen)_2Cl_2] \cdot 2H_2O$ (0.5 mmol, 0.284 g), PMIP (0.5 mmol, 0.155 g), ethanol (10 ml), and water (5 ml) was refluxed under argon for 2 h to give a clear red solution. After most of the ethanol solvent was removed under reduced pressure, a red precipitate was obtained by dropwise addition of a saturated aqueous $NaClO_4$ solution. The product was purified by column chroma-

---

[1]Selected data for PMIP: Anal. Found: C, 77.26; H, 4.63; N, 17.92%. Calc. for $C_{20}H_{14}N_4$: C, 77.42; H, 4.52; N, 18.06%). ^{1}H NMR (DMSO-d_6): δ13.56 (b, 1H), 9.03 (d, 2H), 8.95 (d, 2H), 8.21 (d, 2H), 7.82 (q, 2H), 7.41 (d, 2H), 2.42 (s, 3H). m/z 311 ($[M+1]^+$). For $[Ru(phen)_2PMIP](ClO_4)_2 \cdot H_2O$: Anal. Found: C, 53.68; H, 3.19; N, 11.13%. Calc. for $C_{44}H_{32}Cl_2N_8O_9Ru$: C, 53.44; H, 3.24; N, 11.34%). λ_{max} (nm) (ϵ, M^{-1} cm^{-1}) (water). 454 (13,940), 279.5 (5,469), 263 (71,580). ^{1}H NMR (DMSO-d_6): δ 9.06 (d, 2H), 8.77 (d, 4H), 8.39 (d, 4H), 8.21 (d, 2H), 8.12 (d, 2H), 8.07 (d, 2H), 8.00 (d, 2H), 7.79 (m, 2H), 7.76 (m, 4H), 7.47 (d, 2H), 2.43 (s, 3H). m/z 772 ($[M-2ClO_4^- +1]^{2+}$), 871 ($[M-ClO_4^-]^+$).
[2]Cautionary note: Perchlorate salts of metal complexes with organic ligands are potentially explosive, and only small amounts of the material should be prepared and handled with great care

tography on alumina using acetonitrile–toluene (1:1 v/v) as eluent and then dried in vacuo. Yield, 0.316 g, 64%.

Materials

Both yeast tRNA and CT DNA were obtained from Sigma (Sigma Chemical Co., St. Louis, MO, USA). CT DNA was purified by ethanol precipitation and centrifugal dialysis. The dialysis membrane was purchased from Union Carbide Corporation (Piscataway, NJ, USA) and treated by means of the general procedure before use [35]. Yeast tRNA and CT DNA were dissolved in the corresponding buffer before use with appropriate concentration to be stored at 4°C, and used not more than 1 and 2 days, respectively. Solutions of yeast tRNA and CT DNA gave ratios of UV absorbance at 260 and 280 nm of over 2.0 and 1.8–1.9 respectively, indicating that both nucleic acids were fully free of protein [36]. The concentrations of yeast tRNA and CT DNA solutions were determined at 260 nm by absorption spectroscopy using molar absorption coefficients of 7,700 M^{-1} cm^{-1} for yeast tRNA [37] and 6,600 M^{-1} cm^{-1} for CT DNA [38]. All chemicals used were made in China and of analytical grade. The following buffers were used for the preparation of reagent solutions. 5 mM Tris–HCl buffer (pH 7.2) containing 50 mM NaCl was used for all spectroscopic studies and viscosity measurements of DNA binding of the complex. To avoid the degeneration of RNA induced by metal ions, 5 mM Tris–HCl buffer (pH 7.2) containing 50 mM NaCl and 0.1 mM EDTA (pH 7.2) was used for RNA binding experiments except for ITC measurements. Because the heat effects of ionization and dilution of Tris–HCl buffer were too large to measure the binding heat effect exactly, 30 mM HEPES (Amresco Chemical Co., Solon, OH, USA) buffer (pH 7.2) containing 0.1 mM EDTA was used for all ITC experiments.

UV-vis spectroscopy

UV and visible spectra were measured at 25°C using a UV-2501PC Probe spectrophotometer (Shimadzu, Kyoto, Japan). In order to eliminate the absorbance of nucleic acid itself, an equal amount of yeast tRNA or CT DNA was added into the sample cell containing the Ru(II) polypyridyl complex and the reference cell. The binding constant (K_b) of the complex to nucleic acid was determined from Eq. 1 [39, 40] through a non-linear least-squares plot of ΔA versus the total concentration of nucleic acid (P_t) using MicroCal ORIGIN software. where ΔA is the absorbance at 263 nm for the complex alone minus that for the complex with nucleic acid,

ΔA_{max} is the maximal change of the absorbance difference reached at saturation, and L_t is the total concentration of the Ru(II) complex.

Fluorescence spectroscopy

Fluorescence emission spectra were determined at 25°C using a RF-5301PC fluorescence spectrometer (Shimadzu, Kyoto, Japan). Each spectrum was scanned for three times to acquire the final fluorescence emission spectra. The binding constant of the complex interacting with CT DNA can be derived from the emission spectra using the fluorescence titration method [41]. The binding data obtained from the fluorescence emission spectra were fitted to McGhee and Von Hippel equation [42] to acquire the binding constant K_b.

For the steady-state fluorescence-quenching experiment on CT DNA binding of the complex using $[Fe(CN)_6]^{4-}$ as a quencher, according to the Stern–Volmer equation [43], we have

$$F_0/F = 1 + K_{SV}[Q] \qquad (2)$$

Here, F_0 and F are the fluorescence intensities of the complex in the absence and presence of $[Fe(CN)_6]^{4-}$, respectively, and $[Q]$ is the concentration of the quencher $[Fe(CN)_6]^{4-}$, and K_{SV} is the Stern–Volmer quenching constant which is a measure of the efficiency of fluorescence quenching by $[Fe(CN)_6]^{4-}$.

Viscosity measurements

Viscosities were determined at 28°C using an Ubbdlodhe viscometer (Shanghai Experimental Reagent Co., Shanghai, China). CT DNA samples were prepared by sonication and linearized to an approximate average length of 200 bp in order to minimize complexities arising from DNA flexibility [44]. Flow time was measured with a digital stopwatch. Each sample was measured three times and an average flow time was calculated. Viscosity values were calculated from the observed flow time of DNA-containing solutions ($t > 100$ s) corrected for the flow time of buffer alone (t_0), $\eta = t - t_0$.

Isothermal titration calorimetry

ITC experiments on the interaction of the Ru(II) polypyridyl complex with yeast tRNA and CT DNA in 30 mM HEPES buffer at pH 7.2 were carried out at 25°C using a VP-ITC titration calorimetry (MicroCal, Northampton, MA, USA). All solutions were thoroughly

$$\Delta A = \frac{\Delta A_{max} * [(L_t + P_t + 1/K_b) - \sqrt{(L_t + P_t + 1/K_b)^2 - (4L_t P_t)}]}{2L_t} \qquad (1)$$

degassed before use by stirring under vacuum. Before each experiment, the ITC sample cell was washed several times with HEPES buffer. The sample cell was loaded with 1.43 ml of yeast tRNA or CT DNA solution and the reference cell contained doubly distilled water. Titration was carried out using a 250-μl syringe filled with the complex solution, with stirring at 300 rpm. Injections were started after baseline stability had been achieved. A titration experiment consisted of 28 consecutive injections of 10-μl volume and 20-s duration each, with a 5-min interval between injections. Heats of dilution of the complex were determined by injecting the complex solution into the buffer alone and the total observed heats of binding were corrected for the heat of dilution. The heat released by dilution of yeast tRNA or CT DNA in the cell is negligible. At least two titration experiments were performed for each sample set to evaluate reproducibility. The resulting data were fitted to a single set of identical sites model using MicroCal ORIGIN software supplied with the instrument, and the standard molar enthalpy change for the binding, $\Delta_b H_m^0$, the binding constant, K_b, and the binding stoichiometry, n, which presents the number of bases covered by each complex, were thus obtained. The standard molar free energy change, $\Delta_b G_m^0$, and the standard molar entropy change, $\Delta_b S_m^0$, for the binding reaction were calculated by the fundamental equations of thermodynamics [26, 32]:

$$\Delta_b G_m^0 = -RT \ln K_b \tag{3}$$

$$\Delta_b S_m^0 = \frac{\Delta_b H_m^0 - \Delta_b G_m^0}{T} \tag{4}$$

Equilibrium dialysis and CD spectroscopy

Equilibrium dialysis was carried out in the dark and held at 4°C for 24 h with 5 ml of yeast tRNA or CT DNA (1.0 mM) sealed in a dialysis bag and 10 ml of the Ru(II) polypyridyl complex (100 μM) outside the bag. The CD spectra of the dialysates of the Ru(II) complex were measured with a JASCO J-715 spectropolarimeter (Jasco Corporation, Tokyo, Japan) using a 0.1-cm path length square cell for the 220–350 nm wavelength region at 25°C. The bandwidth was 1 nm and the response time was 1 s. For each CD spectrum, the number of scans was set to 3, and spectral data were collected at 0.1-nm intervals with a scan speed of 200 nm min^{-1}. Both yeast tRNA and CT DNA were dialyzed thoroughly prior to the experiments. For the equilibrium dialysis and CD studies, blank experiment of the complex were also been carried out, and did not show obvious CD signal.

Results

UV-vis spectroscopic studies

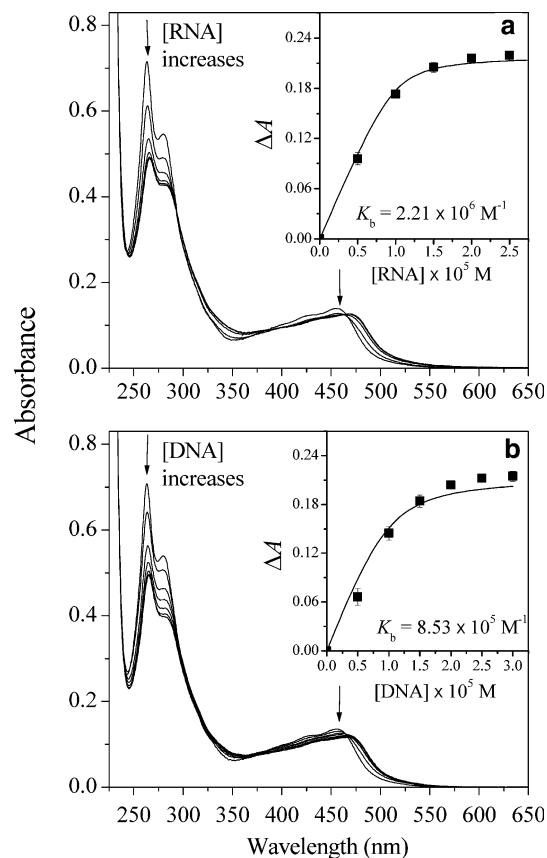Figure 2 shows the UV and visible spectra of complex [Ru(phen)₂PMIP]$^{2+}$ titrated with yeast tRNA and CT

Fig. 2 UV and visible spectra of complex [Ru(phen)₂PMIP]$^{2+}$ upon the addition of yeast tRNA (**a**) and CT DNA (**b**). **a**, *Arrow* represented the concentration of yeast tRNA increased gradually from 0 (*top*) to 25.0 μM (*bottom*). Inset: plot of ΔA versus [RNA] for the titration of the Ru(II) polypyridyl complex with yeast tRNA. **b** *Arrow* represented the concentration of CT DNA increased gradually from 0 (*top*) to 30.0 μM (*bottom*). Inset: plot of ΔA at 263 nm versus [DNA] for the titration of the Ru(II) polypyridyl complex with CT DNA. The *filled squares* were the experimental data and the *solid lines* represented the best fit. The concentrations of the Ru(II) complex was 10.0 μM. Experiments were performed at 25°C in 5 mM Tris–HCl buffer at pH 7.2. Data are expressed as mean ± SD. ($n = 3$)

DNA. The UV-vis spectra of the Ru(II) polypyridyl complex mainly consist of two resolved bands. The low energy absorbance band centered at ~ 455 nm is assigned to metal-to-ligand charge transfer (MLCT) transition and the other band centered at 263 nm is attributed to intraligand (IL) π–π* transition by comparison with the spectra of other Ru(II) polypyridyl complexes [45]. As can be seen from Fig. 2, with the increase of the concentration of yeast tRNA or CT DNA, the UV-vis spectra of the complex showed clearly hypochromism and red shift in all absorbance bands. For yeast tRNA binding of the complex, the UV-vis spectra indicated that the addition of yeast tRNA to the complex yielded hypochromism about 31.6 and 9.4%, and red shifts of 3.0 and 14.5 nm at a molar ratio of yeast tRNA to the complex of 2.5 in the IL band at 263 nm and MLCT band at 454 nm respectively. For CT DNA binding of the complex, upon increasing CT
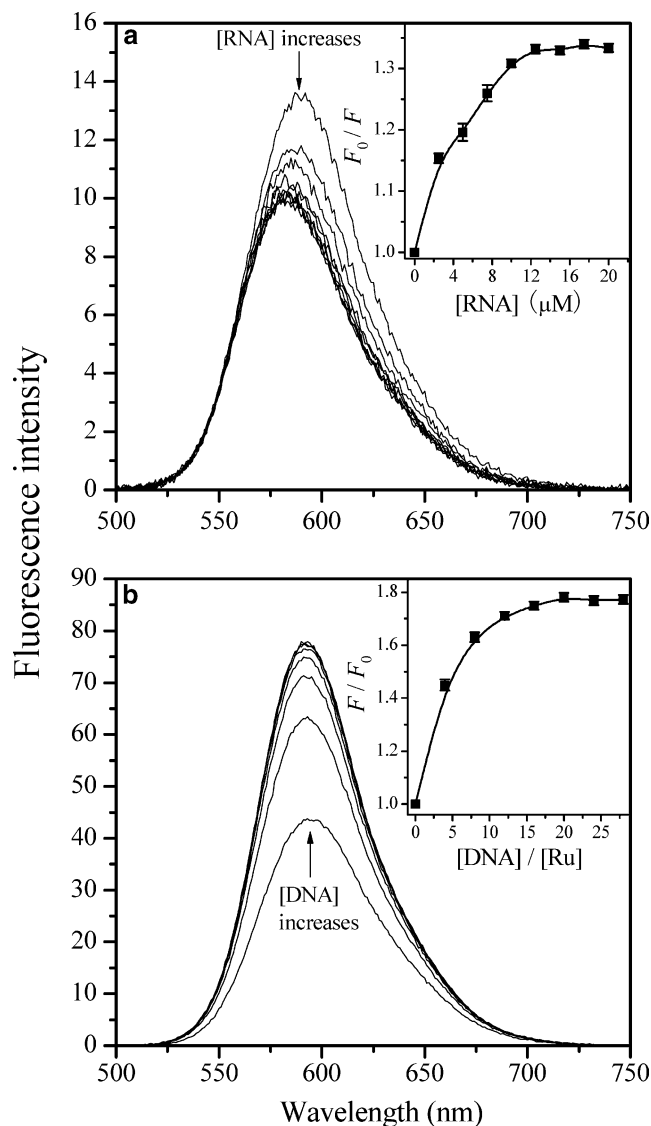
Fig. 3 Fluorescence emission spectra of complex [Ru(phen)$_2$P-MIP]$^{2+}$ in the presence of yeast tRNA (**a**) and CT DNA (**b**). **a**, *Arrow* represented the concentration of yeast tRNA increased gradually from 0 (*top*) to 20.0 μM (*bottom*). The concentrations of the Ru(II) polypyridyl complex was 5.0 μM, and the slit width of 3.0 nm was used for both the excitation and emission beams. Inset: Stern–Volmer plot of the quenching of fluorescence of the Ru(II) complex by yeast tRNA. **b**, *Arrow* represents the concentration of CT DNA increased gradually from 0 (*bottom*) to 200 μM (*top*). The concentrations of the Ru(II) complex was 10.0 μM, and the slit widths of 1.5 and 3.0 nm were used for the excitation and emission beams respectively. Inset: plot of relative fluorescence intensity against the molar ratio of CT DNA to the Ru(II) polypyridyl complex. The *filled squares* represented the experimental data. Measurements were carried out at 25°C in 5 mM Tris–HCl buffer at pH 7.2. Data are expressed as mean ± SD. (*n* = 3)

To compare quantitatively the affinity of the complex binding to yeast tRNA with that of CT DNA (the insets of Fig. 2), the values of K_b of 2.21×10^6 and 8.53×10^5 M^{-1} for yeast tRNA and CT DNA binding of the complex were determined by fitting the binding data obtained from the absorbance spectra at 263 nm according to Eq. 1.

Fluorescence spectroscopic studies

Upon excitation using a wavelength of 460 nm, complex [Ru(phen)$_2$PMIP]$^{2+}$ can emit fluorescence in Tris–HCl buffer with a maximum wavelength of about 590 nm. The results of the fluorescence titration for the Ru(II) polypyridyl complex with yeast tRNA and CT DNA are shown in Fig. 3. For yeast tRNA binding of the complex, the fluorescence intensity of the complex decreased gradually upon the addition of yeast tRNA (Fig. 3a). The hypochromism of the peak reached as high as 24.9% with a blue shift of 8.0 nm at a molar ratio of yeast tRNA to the complex of 3.0. The change in emission for yeast tRNA titration was smaller compared with that for CT DNA. The inset of Fig. 3a shows a Stern–Volmer plot of the quenching of fluorescence of the Ru(II) complex by yeast tRNA, where F_0 and F are the fluorescence intensities in the absence and presence of yeast tRNA. As shown in the inset of Fig. 3a, at higher yeast tRNA concentrations, the quenching curve bended downward obviously and went up slowly, reaching a comparatively saturated situation at the molar ratio of yeast tRNA to the complex of about 3.0. In contrast, for CT DNA binding of the complex, the fluorescence intensity of the complex increased with the increase of CT DNA concentration, reaching a maximum at a molar ratio of CT DNA to the complex of 20, at which there is a 1.8-fold increase in the fluorescence intensity of the complex compared with that in the absence of CT DNA (Fig. 3b). The value of K_b of $4.7 \pm 0.3 \times 10^5$ M^{-1} was determined by fitting the binding data obtained from the fluorescence spectra at 593 nm according to McGhee and Von Hippel equation.

The Stern–Volmer plots of F_0/F versus $[Q]$ for steady-state fluorescence-quenching experiments of CT DNA binding of the complex using [Fe(CN)$_6$]$^{4-}$ as a quencher is shown in Fig. 4. As shown in Fig. 4, in the absence of CT DNA, the Ru(II) complex was quenched by [Fe(CN)$_6$]$^{4-}$ efficiently, resulting in a linear Stern–Volmer plot with a slope of 5.39. In the presence of CT DNA, however, the slope of the plot decreased remarkably, reaching almost zero (0.03).

Viscosity studies

The effects of complex [Ru(phen)$_2$PMIP]$^{2+}$ on the viscosity of CT DNA are shown in Fig. 5. This type of viscosity experiment works because intercalation changes the end-to-end length of the linear DNA. Data were
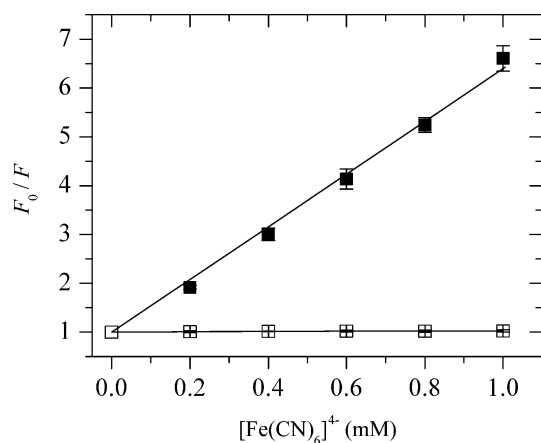
DNA concentration, the hypochromism in the IL band reached as high as 30.3% at 263 nm with a 2-nm red shift at a molar ratio of CT DNA to the complex of 3. The MLCT band at 455 nm showed hypochromism about 14.2% and a red shift of 11 nm under the same experimental conditions.

Fig. 4 Stern–Volmer plots of the quenching of fluorescence of complex $[Ru(phen)_2PMIP]^{2+}$ by $[Fe(CN)_6]^{4-}$ in the absence (*filled square*) and presence (*open square*) of CT DNA. The concentrations of CT DNA and the Ru(II) polypyridyl complex were 160 and 4 μM, respectively. Measurements were carried out at 25°C in 5 mM Tris–HCl buffer at pH 7.2. Data are expressed as mean ± SD. ($n = 3$)

Fig. 5 Effects of increasing concentrations of complex $[Ru(phen)_2PMIP]^{2+}$ on the relative viscosities of CT DNA at 28°C in 5 mM Tris–HCl buffer at pH 7.2. The concentrations of CT DNA was 0.50 mM, and the molar ratios of the Ru(II) polypyridyl complex to CT DNA were 0.02, 0.04, 0.06, and 0.08, respectively. Data are expressed as mean ± SD. ($n = 3$)

presented as $(\eta/\eta_0)^{1/3}$ versus the molar ratio of the Ru(II) complex to CT DNA [46], where η and η_0 are the viscosities of CT DNA in the presence and absence of the complex respectively. As shown in Fig. 5, with the increase of the concentration of the complex, the relative viscosity of CT DNA increased steadily. On the other hand, no obvious change in flow time was observed for yeast tRNA in the presence of the complex.

Thermodynamic analysis of the binding of a Ru(II) complex to yeast tRNA and CT DNA using ITC

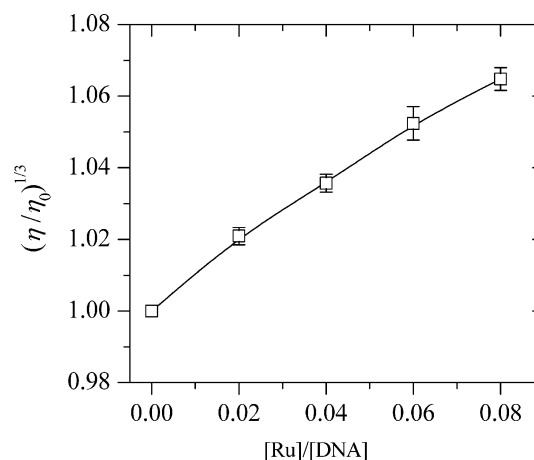ITC profiles for the binding of complex $[Ru(phen)_2PMIP]^{2+}$ to both yeast tRNA and CT DNA at 25°C in 30 mM HEPES buffer at pH 7.2 are shown in Fig. 6. The top panels in Fig. 6 show representatively raw ITC curves resulting from the injections of the Ru(II) complex into a solution of yeast tRNA (Fig. 6a) and CT DNA (Fig. 6c). The titration curves displayed that both the bindings of the complex to yeast tRNA and CT DNA were exothermic, resulting in negative peaks in the plots of power versus time. The bottom panels in Fig. 6 show the plot of the heat evolved per mole of the Ru(II) complex added, corrected for the heat of Ru(II) complex dilution, against the molar ratio of the Ru(II) complex to yeast tRNA (Fig. 6b) and CT DNA (Fig. 6d). The calorimetric data were fitted to a single set of identical sites model and the model employed was the only one yielding a reasonable fitting of

Fig. 6 ITC profiles for the binding of complex $[Ru(phen)_2PMIP]^{2+}$ to yeast tRNA and CT DNA at 25°C in 30 mM HEPES buffer at pH 7.2. The top panels (**a** and **c**) represent the raw data for sequential 10- μL injections of the Ru(II) polypyridyl complex (100 μM) into yeast tRNA (25.0 μM) and CT DNA (25.0 μM), respectively. The bottom panels (**b** and **d**) show the plot of the heat evolved (kcal) per mole of the Ru(II) complex added, corrected for the heat of Ru(II) complex dilution, against the molar ratio of the Ru(II) complex to yeast tRNA and CT DNA, respectively. The data (*filled square*) were fitted to a single set of identical sites model and the *solid line* represented the best fit
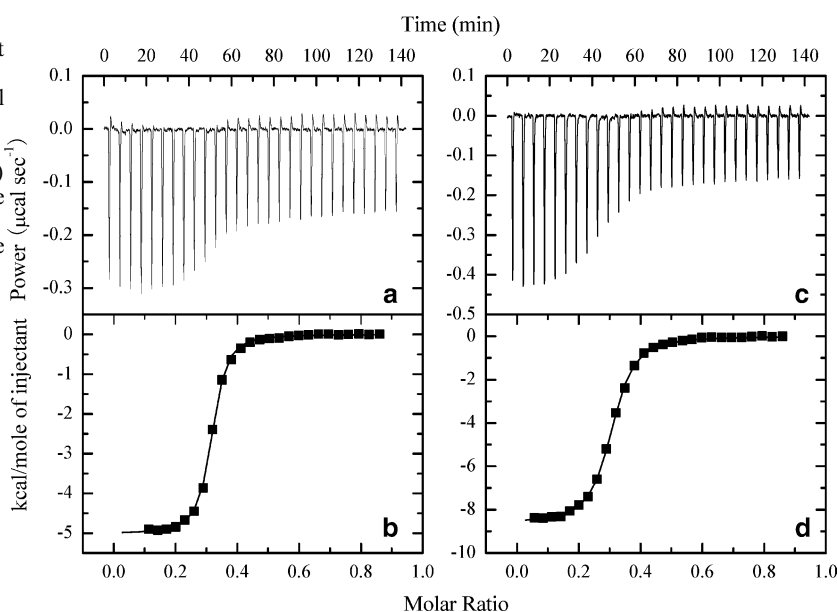
Table 1 Thermodynamic parameters for the binding of complex [Ru(phen)$_2$PMIP]$^{2+}$ to yeast tRNA and CT DNA measured by ITC at 25°C in 30 mM HEPES buffer at pH 7.2

Nucleic acids	$K_b \times 10^{-7}$ (M^{-1})	n (bases/complex)	$\Delta_b H_m^0$ (kcal mol^{-1})	$\Delta_b G_m^0$ (kcal mol^{-1})	$\Delta_b S_m^0$ (cal mol^{-1} K^{-1})
Yeast tRNA	2.30 ± 0.12	3.270 ± 0.007	−5.02 ± 0.02	−10.04 ± 0.03	16.9 ± 0.17
CT DNA	0.887 ± 0.032	3.360 ± 0.008	−8.62 ± 0.03	−9.48 ± 0.02	2.88 ± 0.17

Thermodynamic parameters, K_b, $\Delta_b H_m^0$, and n, were determined using a single set of identical sites model. The standard molar binding free energy ($\Delta_b G_m^0$) and the standard molar binding entropy ($\Delta_b S_m^0$) for the binding reactions were calculated using Eqs. 3 and 4 respectively. Data are expressed as mean ± S.D. (n = 2–3)

the experimental data. The thermodynamic parameters for both binding reactions obtained at 25°C were summarized in Table 1. As shown in Table 1, the interaction of the complex with yeast tRNA was driven by a moderately favorable enthalpy decrease in combination with a moderately favorable entropy increase, while the binding of the complex to CT DNA was driven by a large favorable enthalpy decrease with a less favorable entropy increase.

Enantioselective binding studies

The CD spectra in the UV region of 220–350 nm for complex [Ru(phen)$_2$PMIP]$^{2+}$ after its racemic solution had been dialyzed against yeast tRNA and CT DNA are shown in Fig. 7. As shown in Fig. 7, both dialysates of the Ru(II) complex dialyzed against yeast tRNA and CT DNA showed CD signals with a positive peak at about 245 nm and a negative peak at about 300 nm, and the CD signals for the dialysate of the complex dialyzed

Fig. 7 CD spectra of the dialysates of complex [Ru(phen)$_2$P-MIP]$^{2+}$ after dialysis against yeast tRNA (*red*) and CT DNA (*blue*) for 24 h. The concentrations of yeast tRNA, CT DNA, and the Ru(II) polypyridyl complex were 1.0, 1.0, and 0.10 mM, respectively. Experiments were performed at 25°C

against yeast tRNA were much stronger than those for the complex dialyzed against CT DNA.

Discussion

Ru complexes, modeled by the structure of other typical transition metal compounds like cisplatin, have been drawing scientists' interests for their potentials on developing anticancer drugs [47]. Such complexes have been utilized as DNA structural probes to investigate nucleic acid structure, DNA molecular light switches [48], DNA cleavage agents, and new therapeutics. The common features of these complexes are that the molecule has a high affinity for double-stranded DNA [6–8, 49]. Some Ru complexes appear to be selectively toxic to tumors by being activated by reduction by the tumor itself to bind to nucleic acids [50].

Comparing the hypochromism of the UV-vis spectra for both yeast tRNA and CT DNA binding of complex [Ru(phen)$_2$PMIP]$^{2+}$ with that of CT DNA binding of its parent complex [Ru(phen)$_3$]$^{2+}$ (hypochromism in MLCT band at 445 nm is 12% and the red shift is 2 nm) [51], which interacts with CT DNA through a semi-intercalation or quasi-intercalation [13], and considering that the UV-vis spectrum of [Ru(bpy)$_3$]$^{2+}$ (bpy = 2,2′-bipyridine), a typical electrostatic binding complex, has been demonstrated to be unchanged upon the addition of CT DNA [14], these spectral characteristics obviously suggest that both yeast tRNA and CT DNA binding of the Ru(II) complex used in this paper are most likely through a mode that involved a stacking interaction between the aromatic chromophore and the base pairs of yeast tRNA and CT DNA. Comparing the binding constants obtained with those of typical DNA-intercalative Ru(II) complexes (1.1–4.8×10^{-4} M^{-1}) [48] and the parent complex [Ru(phen)$_3$]$^{2+}$ (5.5×10^3 M^{-1}) [52], we can deduce that both binding modes of the Ru(II) complex to yeast tRNA and CT DNA are most likely intercalation, that is, the PMIP ligand of the complex intercalates into the double-helical regions of yeast tRNA as it interacts with CT DNA. Also, the characteristics of UV and visible spectra, as well as the binding constants obtained demonstrate that yeast tRNA binding of the complex is stronger than CT DNA binding. A possible explanation for this observation may be due to the A-form configuration and the L-shaped tertiary
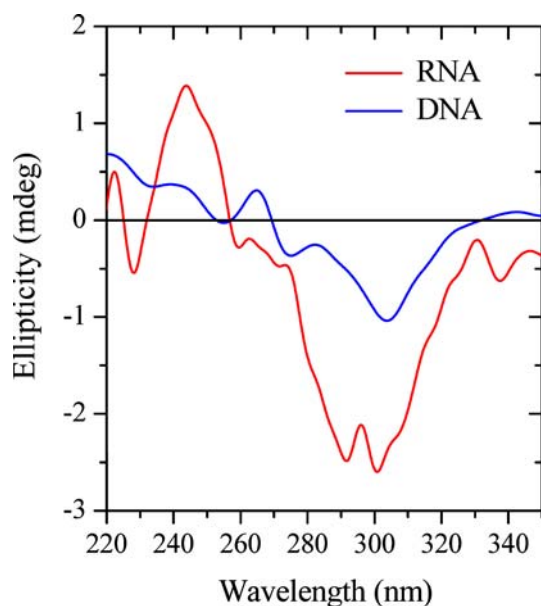
structure of yeast tRNA, in which the major groove is wide and shallow, thus its base pairs are well exposed and can be attacked by complexes easily. In addition, the complex may bind to the bugle region of yeast tRNA and that may be another reason why RNA binding affinity of the complex is greater.

The results from fluorescence titration method for CT DNA binding show that the Ru(II) complex used interacts with CT DNA strongly and is protected by CT DNA efficiently, since the hydrophobic environment inside the DNA helix reduces the accessibility of solvent water molecules to the complex and the complex mobility is restricted at the binding sites, leading to a decrease of the vibrational modes of relaxation. The value of K_b of $4.7 \pm 0.3 \times 10^5$ M^{-1} obtained from fluorescence titration method is comparable to that for a similar complex [Ru(bpy)$_2$MCP]$^{2+}$ (1.8×10^5 M^{-1}, MCP = 2-(3-chlorophenyl)imidazo[4,5-f]1,10-phenanthroline) [53] measured by the same method. For the steady-state fluorescence-quenching experiments of CT DNA binding of the Ru(II) complex, the curvature of the quenching curve reflects different degrees of protection or relative accessibility of bound cations, and a larger slope for the Stern–Volmer plot parallels a poorer protection and weaker binding. The efficiency of quenching of the Ru(II) complex bound to DNA by [Fe(CN)$_6$]$^{4-}$ is decreased extremely relative to that of the free complex. This may be explained by the fact that the bound cations of the complex are protected effectively from the anionic water-bound quencher by the array of negative charges along the DNA phosphate backbone, and that the complex can interact strongly with DNA. On the other hand, the results from fluorescence titration method for yeast tRNA binding suggest that yeast tRNA can partially quench the fluorescence of the Ru(II) complex. This quenching of fluorescence of the Ru(II) complex by yeast tRNA is most probably due to electron or energy transfer between the Ru(II) complex and yeast tRNA caused by a stronger interaction of the complex with yeast tRNA [54]. In addition, the change in emission for yeast tRNA titration was small, which could contribute to the difficulties in utilizing the Stern–Volmer plot at higher yeast tRNA concentrations.

Hydrodynamic measurements sensitive to length changes (i.e., viscosity and sedimentation) are regarded as the most critical tests of a binding model in solution in the absence of crystallographic structural data [43, 55]. For DNA binding of a complex, classical intercalation model demands that the DNA helix lengthen as base pairs are separated to accommodate the bound ligand, leading to an increase in DNA viscosity. The relative viscosity of CT DNA increases with the increase of the concentration of the Ru(II) complex, indicating that the Ru(II) complex binds to DNA through a classical intercalation mode. Such a result is consistent with that obtained from the UV-vis and fluorescence spectroscopic studies in this paper. In contrast, since yeast tRNA is not linear, viscometry, an effective method for studying the interaction mode of metal complexes with

DNA, cannot be used to study the interaction between yeast tRNA and metal complexes.

From the data in Table 1, we can find the following features worthy of note. Firstly, the binding constants of complex [Ru(phen)$_2$PMIP]$^{2+}$ interacting with yeast tRNA and CT DNA obtained from our ITC experiments are comparable to those observed for RNA and DNA binding of some drug molecules by the same method, such as K_b of 3.7×10^7 and 1.7×10^7 M^{-1} for the first RNA binding site of paromomycin [32] and ribostamycin [31] respectively, and K_b of $\sim 10^6$ M^{-1} for DNA binding of intercalated drug molecules [56]. The binding stoichiometry indicates that per complex binds to about three RNA or DNA bases, which is also similar to those of some other Ru(II) polypyridine complexes [55, 57] and drugs [32, 56, 58].

Secondly, the binding constants determined by ITC, by UV-vis spectroscopy, and by fluorescence spectroscopy are different. This is not without precedent. For example, for the interaction of complex [Ru(phen)$_3$]$^{2+}$ with CT DNA, the binding constant determined by equilibrium dialysis experiments is 6.2×10^3 M^{-1} [59], but for its enantiomers, the binding constants obtained from fluorescence spectroscopy with McGhee–Von Hippel method are 4.9×10^4 for its Δ form and 2.8×10^4 M^{-1} for the Λ form [43], and 1.8–3.0×10^6 M^{-1}, 0.3–4.2×10^6 M^{-1} for the Δ and Λ isomers at different concentrations using the method suggested by Coggan et al. [57]. Moreover, for the enantiomer Δ-[Ru(phen)$_2$DPPZ]$^{2+}$ (DPPZ = dipyrido[3,2-a:2',3'-c]phenazine) interacting with CT DNA, the binding constant determined by Hiort et al. (6.0×10^7 M^{-1}) [60] from fluorescence titration method is also different from that measured by Haq et al. (3.2×10^6 M^{-1}) [61] using the same method but with different model. These differences should be caused by the different measurements and the different calculation methods. Furthermore, we should be aware of the importance of the ionic strength of the buffer for the binding of charge ligands to DNA [62, 63], which in part explains the much higher binding constants obtained from ITC in which a different buffer with different ionic strength was used. However, although the binding constants obtained from our ITC experiments are about one order of magnitude higher than those obtained from UV-vis spectroscopy, both sets of binding constants show that yeast tRNA binding of complex [Ru(phen)$_2$PMIP]$^{2+}$ is 2.6-fold stronger than CT DNA binding of the complex. These results suggest that we can compare RNA or DNA binding strength of one complex with that of the others using binding constant only obtained from the same method with the same model.

Thirdly, ITC experiments show that the interaction of the Ru(II) complex with yeast tRNA is driven by a moderately favorable enthalpy change in combination with a moderately favorable entropy change, while the binding of the complex to CT DNA is driven by a more favorable enthalpy change with a less favorable entropy change. These can be explained by the fact that both

binding modes of complex [Ru(phen)$_2$PMIP]$^{2+}$ to yeast tRNA and CT DNA are intercalation. Once the Ru(II) complex intercalates into the adjacent base pairs of yeast tRNA or CT DNA, a variety of noncovalent molecular interactions, such as stacking interactions of the aromatic ligand in the complex with the base pairs of RNA or DNA, specific hydrogen bonds and van der Waals interactions between the complex and RNA or DNA, may occur [64]. Each of these weak interactions leads to negative enthalpy change [65], and the apparent enthalpy decrease should be the summation of all of these molecular interactions [56]. On the other hand, the favorable entropy change should result from the relaxation of supercoiled yeast tRNA with the L-shaped tertiary structure or CT DNA induced by the intercalation of the complex [66], the liberation of structured water from interacting surfaces, and/or the release of counterions upon binding of positively charged complexes [56, 58]. The increase in entropy for yeast tRNA binding of the complex is more favorable than that for CT DNA binding, suggesting that the extent of relaxation of yeast tRNA induced by the intercalation of the complex may be larger than that of CT DNA owing to its stronger interaction with the complex. ITC results herein further support the conclusion that yeast tRNA binding of the complex is stronger than CT DNA binding reached by UV-vis spectroscopy and fluorescence spectroscopy.

The enantiospecific binding of complex [Ru(phen)$_2$PMIP]$^{2+}$ to yeast tRNA or CT DNA can be observed clearly from CD spectra. The presence of CD signals indicates enrichment of the enantiomer binding less favorably to yeast tRNA or CT DNA. From our CD experiments, we may deduce that, although the Ru(II) complex used has not been resolved into its pure enantiomers, and we cannot determine which enantiomer binds to yeast tRNA and CT DNA enantioselectively experimentally, it is certain that the same isomer of the complex has a special preference for both yeast tRNA and CT DNA binding, and that the complex is a better candidate for an enantioselective binder to yeast tRNA than to CT DNA. According to the proposed binding model [64, 67], the Δ enantiomer of the complex, a right-handed propeller-like structure, will display a greater affinity than the Λ enantiomer with the right-handed CT DNA helix, due to the appropriate steric matching. Although the configuration of CT DNA is different from that of yeast tRNA, both yeast tRNA and CT DNA have the same right-handed helix structure. Therefore, we deduce that the Δ enantiomer of the complex may bind more favorably to both yeast tRNA and CT DNA than the Λ enantiomer does. In addition, the phenomenon that the CD signals for the dialysate of the complex dialyzed against yeast tRNA are much stronger than those for the complex dialyzed against CT DNA may be explained by the fact that yeast tRNA binding of the complex is stronger than CT DNA binding.

In summary, combining the results from UV-vis spectroscopy, fluorescence spectroscopy, viscosity measurements, ITC, equilibrium dialysis, and CD, we conclude that both binding modes of the Ru(II) polypyridyl complex to yeast tRNA and CT DNA are intercalation, RNA binding of the complex is stronger than DNA binding, the Δ enantiomer of the complex may bind more favorably to both CT DNA and yeast tRNA, and the Ru(II) polypyridyl complex is a better candidate for an enantioselective binder to yeast tRNA than to CT DNA. All these experimental results can be explained by the different structure and configuration between yeast tRNA and CT DNA reasonably, suggesting that the configuration and structure of nucleic acids have significant effects on the binding behaviors of metal complexes. Information obtained from the present study can enhance our understanding of the mechanism for the binding of Ru(II) polypyridyl complexes to nucleic acids, and is helpful to the development of nucleic acid molecular probes and new therapeutic regents for some diseases related to viruses such as AIDS and SARS.

References

1. Dupureur CM, Barton JK (1997) Inorg Chem 36:33–43
2. Greguric I, Aldrich-Wright JR, Collins JG (1997) J Am Chem Soc 119:3621–3622
3. Nair RB, Teng ES, Kirkland SL, Murphy CJ (1998) Inorg Chem 37:139–141
4. Liu JG, Ye BH, Li H, Ji LN, Li RH, Zhou JY (1999) J Inorg Biochem 73:117–122
5. Onfelt B, Gostring L, Lincoln P, Nordén B, Onfelt A (2002) Mutagenesis 17:317–320
6. Xu H, Zheng KC, Chen Y, Li YZ, Lin LJ, Li H, Zhang PX, Ji LN (2003) Dalton Trans 2260–2268
7. Xu H, Zheng KC, Deng H, Lin LJ, Zhang QL, Ji LN (2003) New J Chem 27:1255–1263
8. Xu H, Zheng KC, Lin LJ, Li H, Gao Y, Ji LN (2004) J Inorg Biochem 98:87–97
9. Olofsson J, Onfelt B, Lincoln P, Nordén B, Matousek P, Parker AW, Tuite E (2002) J Inorg Biochem 91:286–297
10. Coates CG, Olofsson J, Coletti M, McGarvey JJ, Onfelt B, Lincoln P, Nordén B, Tuite E, Matousek P, Parker AW (2001) J Phys Chem B 105:12653–12664
11. Onfelt B, Lincoln P, Nordén B, Baskin JS, Zewail AH (2000) Proc Natl Acad Sci USA 97:5708–5713
12. Gisselfalt K, Lincoln P, Nordén B, Jonsson M (2000) J Phys Chem B 104:3651–3659
13. Lincoln P, Nordén B (1998) J Phys Chem B 102:9583–9594
14. Yang G, Wu JZ, Wang L, Ji LN, Tian X (1997) J Inorg Biochem 66:141–144
15. Wu JZ, Ye BH, Wang L, Ji LN, Zhou JY, Li RH, Zhou JY (1997) Dalton Trans 1395–1401
16. Xiong Y, He XF, Zou XH, Wu JZ, Chen XM, Ji LN, Li RH, Zhou JY, Yu KB (1999) Dalton Trans 19–23
17. Chu F, Smith J, Lynch VM, Anslyn EV (1995) Inorg Chem 34:5689–5690

538

18. Lim AC, Barton JK (1998) Biochemistry 37:9138–9146
19. Carter PJ, Cheng CC, Thorp HH (1998) J Am Chem Soc 120:632–642
20. Chow CS, Barton JK (1992) Biochemistry 31:5423–5429
21. Xu H, Deng H, Zhang QL, Huang Y, Liu JZ, Ji LN (2003) Inorg Chem Commun 6:766–768
22. Luedtke NW, Hwang JS, Glazer EC, Gut D, Kol M, Tor Y (2002) Chembiochem 3:766–771
23. Luedtke NW, Hwang JS, Nava E, Gut D, Kol M, Tor Y (2003) Nucleic Acids Res 31:5732–5740
24. Liang Y, Du F, Sanglier S, Zhou BR, Xia Y, Van Dorsselaer A, Maechling C, Kilhoffer MC, Haiech J (2003) J Biol Chem 278:30098–30105
25. Weber PC, Salemme FR (2003) Curr Opin Struct Biol 13:115–121
26. Ladbury JE, Williams MA (2004) Curr Opin Struct Biol 14:562–569
27. Cliff MJ, Gutierrez A, Ladbury JE (2004) J Mol Recognit 17:513–523
28. Lobo BA, Davis A, Koe G, Smith JG, Middaugh CR (2001) Arch Biochem Biophys 386:95–105
29. Kaul M, Pilch DS (2002) Biochemistry 41:7695–7706
30. Kaul M, Barbieri CM, Kerrigan JE, Pilch DS (2003) J Mol Biol 326:1373–1387
31. Jin E, Katritch V, Olson WK, Kharatisvili M, Abagyan R, Pilch DS (2000) J Mol Biol 298:95–110
32. Liang Y, Du F, Zhou BR, Zhou H, Zou GL, Wang CX, Qu SS (2002) Eur J Biochem 269:2851–2859
33. Amouyal E, Homsi A, Chambron JC, Sauvage JP (1990) Dalton Trans 1841–1845
34. Sullivan BP, Salmon DJ, Meyer TJ (1978) Inorg Chem 17:3334–3341
35. Barton JK, Dannenberg JJ, Raphael AL (1982) J Am Chem Soc 104:4967–4969
36. Marmur J (1961) J Mol Biol 3:208–214
37. Reichmann ME, Rice SA, Thomas CA, Doty P (1954) J Am Chem Soc 76:3047–3053
38. Meadows KA, Liu F, Sou J, Hudson BP, McMillin DR (1993) Inorg Chem 32:2919–2923
39. Stafshede PW, Guidry J, Horne BE, Landry SJ (2003) Biochemistry 42:4937–4944
40. Milev S, Gorfe AA, Karshikoff A, Clubb RT, Bosshard HR, Jelesarov I (2003) Biochemistry 42:3481–3491
41. Satyanarayana S, Dabrowiak JC, Chaires JB (1992) Biochemistry 31:9319–9324
42. McGhee JD, Von Hippel PH (1974) J Mol Biol 86:469–489
43. Lakowicz JR, Webber G (1973) Biochemistry 12:4161–4170
44. Chaires JB, Dattagupta N, Crothers DM (1982) Biochemistry 21:3933–3940
45. Juris A, Balzani V, Barigelletti F, Campagna S, Belser P, Von Zelewsky A (1988) Coordin Chem Rev 84:85–277
46. Cohen G, Eisenberg H (1969) Biopolymers 8:45–55
47. Novakova O, Chen H, Vrana O, Rodger A, Sadler PJ, Brabec V (2003) Biochemistry 42:11544–11554
48. Zou XH, Ye BH, Li H, Zhang QL, Chao H, Liu JG, Ji LN, Li XY (2001) J Biol Inorg Chem 6:143–150
49. Wang J, Bard AJ (2001) Anal Chem 73:2207–2212
50. Clarke MJ, Zhu F, Frasca DR (1999) Chem Rev 99:2511–2533
51. Xiong Y, Ji LN (1999) Coordin Chem Rev 185–186:711–733
52. Pyle AM, Rehmann JP, Meshoyrer R, Kumar CV, Turro NJ, Barton JK (1989) J Am Chem Soc 111:3051–3058
53. Xiong Y, Zou XH, Wu JZ, Ji LN, Li RH, Zhou JY, Yu KB (1999) Transit Met Chem 24:263–267
54. Watson RT, Desai N, Wildsmith J, Wheeler JF, Kane-Maguire NAP (1999) Inorg Chem 38:2683–2687
55. Satyanarayana S, Dabrowiak JC, Chaires JB (1993) Biochemistry 32:2573–2584
56. Haq I, Ladbury J (2000) J Mol Recognit 13:188–197
57. Coggan DZM, Haworth IS, Bates PJ, Robinson A, Rodger A (1999) Inorg Chem 38:4486–4497
58. Haq I, Ladbury JE, Chowdhry BZ, Jenkins TC, Chaires JB (1997) J Mol Biol 271:244–257
59. Barton JK, Danishefsky AT, Goldberg JM (1984) J Am Chem Soc 106:2172–2176
60. Hiort C, Lincoln P, Nordén B (1993) J Am Chem Soc 115:3448–3454
61. Haq I, Lincoln P, Suh D, Nordén B, Chowdhry BZ, Chaires JB (1995) J Am Chem Soc 117:4788–4796
62. Manning GS (1969) J Chem Phys 51:924–933
63. Record MT Jr, Anderson CF, Lohman TM (1978) Q Rev Biophys 11:103–178
64. Chaires JB (1998) Biopolymers 44:201–215
65. Ross DP, Subramanian S (1981) Biochemistry 20:3096–3102
66. Stubbe J, Kozarich JW (1987) Chem Rev 87:1107–1136
67. Pyle AM, Barton JK (1990) Prog Inorg Chem 38:413–475